コンクリート工学年次論文報告集，Vol.15，No.2，1993

論 文

[2209] Localization Analysis of a Concrete Bar Subjected to Compression

Guo-Xiong YU* and Tada-aki TANABE* [1]

1. INTRODUCTION

A phenomenon that frequently accompanies inelastic deformation is that large strain accumulates inside a band without substantially affecting the strain in the surrounding material. This phenomenon called "localization" emerges as an outcome of the constitutive behavior of the material, and occurs in a wide variety of solids including concrete material. Once localization takes place, large strain can accumulate inside the band and lead to fracture. Being interested in this phenomenon, the authors have started to apply the theory for reinforced concrete and try to capture this phenomenon by finite element method. In this study, we present some result of investigation which is only limited to nonreinforced concrete. The method proposed by Ortiz[1], is used to enhance the performance of general classes of elements in the problems involving strain localization. Numerical studies of two specimens are presented with one material following J_2 theory and the other following the concrete constitutve model proposed by Wu and Tanabe[2]. Throughout the numerical calculation, the determinant of the total tangential stiffness matrix is calculated in order to determine the relation between localization bifurcation phenomenon and other kinds of bifurcation occuring when the determinant of the tangential stiffness matrix is singular.

2. LOCALIZATION CONDITION

The localization condition can be written as

$$A_{jk}(\mathbf{n})m_k = 0, \tag{1}$$

where $A_{jk}(\mathbf{n}) = n_i D_{ijkl} n_l$,$\mathbf{D}$ is the tangent stiffness tensor for a material and $\mathbf{n}$ is the localization direction[3]. By the pair of unit vectors, $\mathbf{m}$ and $\mathbf{n}$(Figure 1), the nature of the discontinuity can be entirely defined. When $\mathbf{m}$ is orthogonal to $\mathbf{n}$, the material in the band deforms in pure shear, when $\mathbf{m}$ is parallel to $\mathbf{n}$, the band undergoes extension normal to the planes of discontinuity and a splitting failure mode results. Thus, for localization to occur along the direction $\mathbf{n}$, the localization matrix $A(\mathbf{n})$ has to have at least one zero eigenvalue. This in turn necessitates

$$f(\mathbf{n}) = det(A(\mathbf{n})) = 0, \tag{2}$$

[1]* Department of Civil Engineering, Nagoya University

which constitutes an alternative form of the localization condition in eq.(1).

3. LOCALIZED DEFORMATION MODES

It is known that when conventional displacement finite element method is used, in order to accurately resolve a narrow shear band, small elements are required, and furthermore, the mesh should be optimally designed so that the element boundaries follow shear band directions, otherwise shear band will be broaden. But by using the method proposed by Ortiz, we can capture the localization phenomenon sharply with rectangular mesh and isoparametric elements without taking explicit account of likely direction of localization. The method is described briefly as follows:

1. For every element in the mesh, the calculation of localization condition is carried on at the reduced quadrature points until the onset of localization.

2. From this point on, suitable deformation modes which exactly reproduce the discontinuous deformation patterns are added to the element where localization is detected. The extra degree of freedom are eliminated at the element level by means of static condensation.

Let us assume that in the element under consideration several bifurcations have been detected resulting in NL localized modes. The geometry of these deformation modes is fully determined by pairs of unit vectors $\{(m_{i\alpha}, n_{i\alpha}), \alpha = 1, 2, ..., NL\}$. We also let ξ_α denote the reduced quadrature point at which the αth localized mode has been detected. Now for each localized mode we defined the functions

$$M^+_{i\alpha}(x) = \begin{cases} m_{i\alpha}\,[\mathbf{n}_\alpha \cdot (\mathbf{x} - \xi_\alpha)] & \mathbf{n}_\alpha \cdot (\mathbf{x} - \xi_\alpha) > 0, \\ 0 & otherwise, \end{cases} \tag{3}$$

$$M^-_{i\alpha}(x) = \begin{cases} -m_{i\alpha}\,[\mathbf{n}_\alpha \cdot (\mathbf{x} - \xi_\alpha)] & \mathbf{n}_\alpha \cdot (\mathbf{x} - \xi_\alpha) < 0, \\ 0 & otherwise, \end{cases} \tag{4}$$

$$M_{i\alpha}(x) = (1 - \lambda_\alpha) M^-_{i\alpha}(x) + \lambda_\alpha M^+_{i\alpha}(x), \tag{5}$$

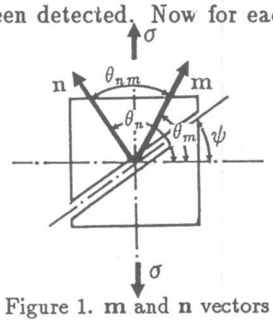

Figure 1. **m** and **n** vectors

where the superindex '+' and '-' refer to the plus side and the minus side of the plane of discontinuity and no sum is implied on the index of α. Adding these shape functions to the element interpolation, the local displacement field becomes

$$u_i(x) = \sum_{\alpha=1}^{N} u_{i\alpha} N_\alpha(x) + \sum_{\alpha=1}^{NL} \gamma_\alpha M_{i\alpha}(x), \tag{6}$$

where $\{\gamma_\alpha, \alpha = 1, 2, ...NL\}$ are the amplitudes of the localized modes and defines a one-parameter family of possible shape function for the localized mode, and it exhibits a jump across the surface of discontinuity. The element strain can be obtained as

$$\begin{aligned} \varepsilon(x) &= \frac{1}{2}(u_{i,j}(x) + u_{j,i}(x)) \\ &= \sum_{a=1}^{NL} \frac{1}{2}(u_{ia} N_{a,j}(x) + u_{ja} N_{a,i}(x)) + \sum_{\alpha=1}^{NL} \frac{1}{2}\gamma_\alpha((M_{i\alpha})_{,j}(x) + (M_{j\alpha})_{,i}(x)). \end{aligned} \tag{7}$$

Let $\mathbf{u}_1$ and $\mathbf{u}_2$ denote the nodal displacement and amplitude γ_α of the additional incompatible modes, respectively. Then eq.(7) can be rewritten as

$$\varepsilon(x) = \mathbf{B}_1 \mathbf{u}_1 + \mathbf{B}_2 \mathbf{u}_2. \tag{8}$$

From eq.(3) to eq.(5) $\mathbf{B}_2$ takes the form of

$$(B_2)_{ij\alpha} = \begin{cases} \frac{1}{2}\lambda_\alpha(m_{i\alpha}n_{j\alpha} + m_{j\alpha}n_{i\alpha}) & \mathbf{n}_\alpha \cdot (x - \xi_\alpha) > 0, \\ -\frac{1}{2}(1-\lambda_\alpha)(m_{i\alpha}n_{j\alpha} + m_{j\alpha}n_{i\alpha}) & \mathbf{n}_\alpha \cdot (x - \xi_\alpha) \leq 0, \end{cases} \tag{9}$$

so that the element strain field exhibits a jump

$$\varepsilon(x) = \varepsilon(x)^+ - \varepsilon(x)^- = \frac{1}{2}\gamma_\alpha(m_{i\alpha}n_{j\alpha} + m_{j\alpha}n_{i\alpha}) \tag{10}$$

across the αth surface of discontinuity. Since the localized modes represent internal degrees of freedom of the element, the $\mathbf{u}_2$ can be eliminated by static condensation.

4. A HARDENING SOFTENING MODEL OF CONCRETE SUBJECTED TO COMPRESSIVE LOADING

A constitutive model for concrete under compressive loading was proposed by Wu and Tanabe[2]. In this model, the failure procedure of concrete material depends on the plastic strain history through a introduced damage parameter ω. The damage parameter was defined as $\omega = \beta \int d\varepsilon_p/\varepsilon_o$, where β is a material constant. $\varepsilon_o = f_c/E_c$, E_c denotes the modulus of elasticity of concrete and f_c is the uniaxial compressive strength.

The yield criterion was defined as

$$f = \sqrt{J_2} + \alpha_f I_1 - k_f = 0, \tag{11}$$

where

$$\alpha_f = \frac{2sin\phi^*}{\sqrt{3}(3 - sin\phi^*)}, \tag{12}$$

$$k_f = \frac{6C^*cos\phi^*}{\sqrt{3}(3 - sin\phi^*)}, \tag{13}$$

$$C^* = Cexp\left[-(m\omega)^2\right], \tag{14}$$

$$\phi^* = \begin{cases} \phi\sqrt{2\omega - \omega^2} & \omega \leq 1, \\ \phi & \omega > 1. \end{cases} \tag{15}$$

In the equation above, m is the material parameter,C and ϕ are the cohesion and internal-friction angle of the concrete. I_1 and J_2 are the first invariant of stress tensor σ_{ij}, and the second invariant of deviatoric stress tensor S_{ij}.Figure 2 is the uniaxial stress-strain relation curve with $\beta = 1.0$,$E_c = 2 \times 10^{10} Pa$, $C = 10^7 Pa$,$\phi = 30°$ and $m = 2.0$.

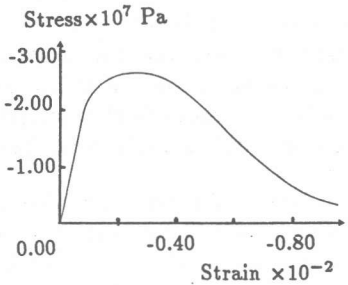

Figure 2. Stress-Strain Curve of Uniaxial Compression

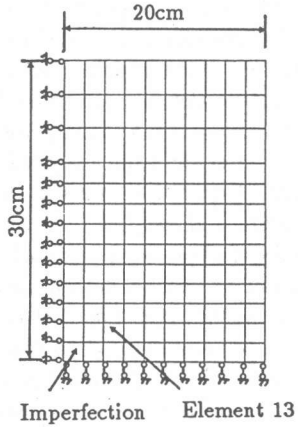

Figure 3. Mesh and Boundary Condition
Thickness 1 cm

5. NUMERICAL EXPERIMENT 1

A rectangular bar following J_2 theory,though hardening and softening character is embeded, is examined in the first numerical study. Figure 3 shows the finite mesh and the boundary conditions. The bar is subjected to prescribed uniform displacements at both ends.Plane

stress condition is assumed. Without imperfection, the bar would result in a state of uniform tension stretch. So a weak element, which E and σ_y is reduced by factor of 100, is introduced to enhance the growth of nonhomogeneity . Figure 4 shows the uniaxial stress-strain relation of the material with $E = 2 \times 10^{11} Pa$ and $v = 0.3$, where E is the Young's modulus and v is the Poission's ratio. The yield stress of the material is taken to be $\sigma_y = 2.4 \times 10^8 Pa$. When the effective plastic strain satisfies the condition $0 < \varepsilon_p^e < 1.2 \times 10^{-3}$, the plastic modulus $H_1 = 2.5 \times 10^{10} Pa$, and when $1.2 \times 10^{-3} < \varepsilon_p^e$, the plastic modulus is changed to $H_2 = 0.0, -1.30 \times 10^{10}$ and $-3.90 \times 10^{10} Pa$, respectively. Figure 5 shows the force and the displacement relation with different H_2 . Through the calculation, it is found that the smaller the value of H_2, the narrower the shear band becomes. At every step, the localization matrix is detected, with $H_2 = -3.90 \times 10^{10} Pa$, all the elements satisfying the localization condition are found within the shear band in which the direction is 45° to the side of the specimen from the imperfection element. All the following results are related to $H_2 = -3.90 \times 10^{10}$Pa.

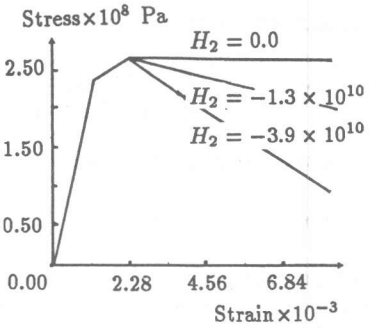

Figure 4. Stress-Strain Curve of Uniaxial Tension

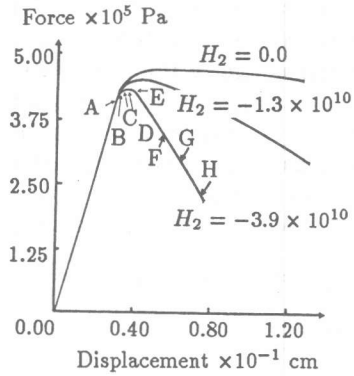

Figure 5. Force-Displacement Curve of Uniaxial Tension

The localization matrix $A(\mathbf{n})$ of each element and the total tangential stiffness matrix are both calculated at every step. At step A (Figure 5) , the first element, in which the determinant of localization matrix turns out to be zero, is detected. After that , the shear band propagates along the direction of 45° to the specimen side until step E. After step E, the determinants of localization of the elements localized previously remain negative or zero, but there are no other elements resulting in localization at all. Figure 6 shows the propagation of the localization, the alphabets inside the elements denote the step shown on Figure 5. At step E , when the shear band goes through the specimen, the minimum eigen value of the total tangential stiffness matrix becomes negative. Figure 7 shows the shape of the deformed mesh and Figure 8 shows the distribution of the effective strain ε_p^e within the specimen. At each step the directions of vectors, n and m , which determine the localization modes, are also calculated. It is found that the direction with normal of n is always about 45° to the side of the specimen, and m is always almost perpendicular to n . Here element 13 (Figure 3) is selected as a representive element of which the determinant of localization matrix $det(A(\mathbf{n}))$ and direction of n and m are recorded at every step. These records are shown by Figure 9 and Table 1. Table 1 shows the value of direction of n and m within the step of A and H. From it, we can see that, within the step of A and E, angle θ_{mn} between n and m is almost equal to 90° which means that element 13 behaves in simple shear mode. After that θ_{mn} decreases gradually; this implies that element 13 changes

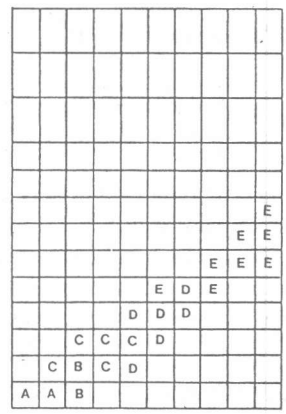

Figure 6. Localization Propagation of Uniaxial Tension

slightly to splitting failure mode from simple shear mode.

6. NUMERICAL EXPERIMENT 2

A rectangular bar with the same finite element mesh and boundary condition as the numerical experiment 1 in section 5 is used, but the material is concrete which follows the constitutive model described in section 4. This time, the bar is subjected to prescribed uniform displacements at both ends. Also, plane stress condition is assumed. The material properties are assumed as $E = 2.0 \times 10^{10} Pa, C = 10^7 Pa$ and $\phi = 30°$. Figure 2 shows the stress-strain curve of uniaxial compression.

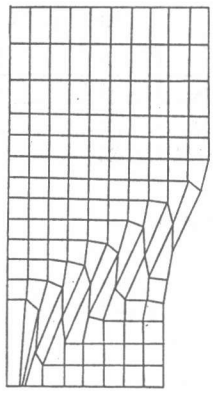

Figure 7. Shape of Deformed Mesh of Uniaxial Tension

First, without an imperfection element, the specimen undergoes a uniform compression with the stress state of uniaxial compression. When compressive stress increases, the localization condition is satisfied in every Gauss point of the specimen. The direction of shear band ψ is equal to 38.0°. The angle θ_{mn} is equal to 89.8°; this means failure is predominantly of shear type. Kupfer and Hilsdorf obtained the localized failure in uniaxial compression at an angle $\psi = 30°$ by experiment[4], but exact uniaxiality is difficult to obtain in the laboratory and thus many investigators report localized failure modes of the type predicted by the method for nearly uniaxial paths.

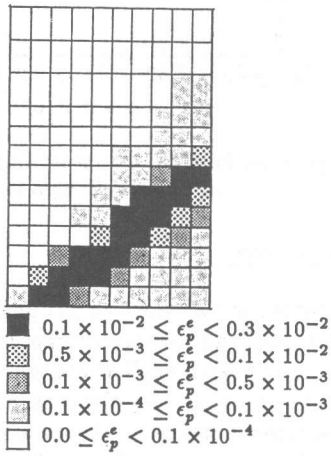

Figure 8. At Step G The Distribution of Effective Plastic Strain

Then, an imperfection element was added into the mesh with Young's modulus E and coefficient of cohesion C reduced by the factor of 100. Figure 9 shows the load and displacement relation curve. Figure 10 shows the propagation of the localized elements. Figure 11 shows the deformed mesh. And again, at the step F, when the shear band develops through the specimen, the eigenvalue of the total tangential stiffness matrix becomes negative. Obviously, step F is beyond the peak point which means that the singularity of total tangential stiffness matrix does not occur at the peak point. This contradicts to the aforementioned case, however, the calculation is carried on by displacement control wherein the load at the top of the bar does not monotonously increase. Table 2 shows the direction of the vector n and m of element 13. Like the J_2 material, the angle of θ_{mn} becomes less,which show the tendency of shifting to splitting failure from pure shear failure mode gradually.

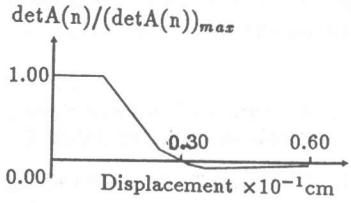

Figure 9. Determinant of Localization Matrix

Table 1. The Direction of Localization of Uniaxial Tension

	A	B	C	D	E	F	G	H
θ_n	134.9	145.8	145.2	144.8	144.5	144.0	142.7	139.2
θ_m	58.5	55.4	56.0	56.7	57.5	58.4	61.0	63.26
θ_{mn}	76.4	90.4	89.2	88.1	87.0	85.5	81.7	76.0

Table 2. The Direction of Localization of Uniaxial Compression

	A	B	C	D	E	F	G
θ_n	144.1	143.8	143.5	143.3	143.0	142.9	142.7
θ_m	55.6	56.0	56.5	56.9	57.4	57.8	58.1
θ_{ms}	88.4	87.8	87.0	86.3	85.6	85.1	84.63

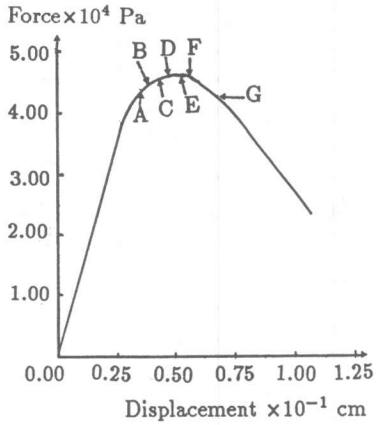

Figure 10. Force-Displacement Curve of Uniaxial Compression

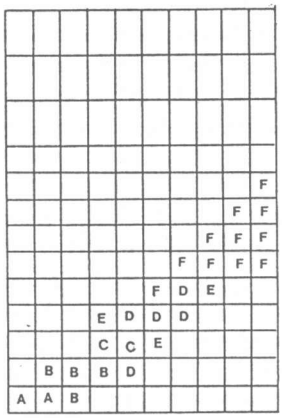

Figure 11. Localization Propagation of Uniaxial Compression

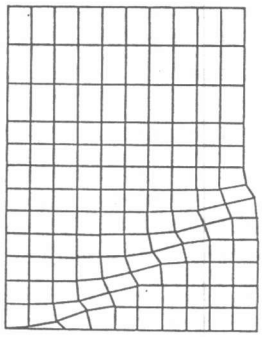

Figure 12. Shape of Deformed Mesh of Uniaxial Compression

7 CONCLUSION

By enhancing the element performance through the method proposed by Ortiz, the localization phenomenon can be captured sharply with rectangular mesh and isoparametric elements without taking explicit account of likely direction of localization. Numerical studies were carried out to capture the localization phenomenon on two different cases, one case is with a specimen obeying J_2 theory and the other with a specimen obeying the concrete constitutive model proposed by Wu and Tanabe. For the concrete specimen obeying that constitutive model and subjected to uniaxial compression, localization of shear type predominates with the shear band occurring 38° with respect to the compressive load direction. For both specimens the eigen value of the total tangential stiffness matrix become negative when shear band develops through the specimen.

REFERENCES

1. M. Ortiz et," A finite element method for localized failure analysis," *Comp. method in App. Mech. and Eng.*, 61(1987) 189-214.

2. Z. Wu and T. Tanabe,"A hardening and softening model of concrete subjected to compressive loading," *Journal of Structure Engineering Architecture Institute of Japan*, Vol.36B,March,1990,153-162.

3. J.R.Rice, "The deformation of plastic deformation,", W.T.Koiter,ed., *Theoretical and applied mechanics*,1976,207-220.

4. Kupfer,H.,H.K.Hilsdorf and H.Rusch,"Behavior of concrete under biaxial stress,", J.ACI, 1969, 66(8)656.